www.czasopisma.pan.pl PAN www.journals.pan.pl

ARCHIVES of FOUNDRY ENGINEERING

ISSN (2299-2944)
Volume 2023
Issue 2/2023

137 – 144

10.24425/afe.2023.144306

19/2

Published quarterly as the organ of the Foundry Commission of the Polish Academy of Sciences

Prediction of Selected Mechanical Properties in Austempered Ductile Iron with Different Wall Thickness by the Decision Support Systems

K. Jaśkowiec [a, b], A. Opaliński [b], P. Kustra [b], D. Jach [c], D. Wilk-Kołodziejczyk [b, a]

[a] Lukasiewicz Research Network-Krakow Institute of Technology, Poland
[b] AGH University of Science and Technology, Department of Applied Computer Science and Modelling, Poland
[c] Kutno Foundry, Poland
* Corresponding author. E-mail address: wilk.kolodziejczyk@gmail.com

Received 16.03.2023; accepted in revised form 22.04.2023; available online 29.06.2023

Abstract

The structure of Austempered Ductile Iron (ADI) is depend of many factors at individual stages of casting production. There is a rich literature documenting research on the relationship between heat treatment and the resulting microstructure of cast alloy. A significant amount of research is conducted towards the use of IT tools for indications production parameters for thin-walled castings, allowing for the selection of selected process parameters in order to obtain the expected properties. At the same time, the selection of these parameters should make it possible to obtain as few defects as possible. The input parameters of the solver is chemical composition Determined by the previous system module. Target wall thickness and HB of the product determined by the user. The method used to implement the solver is the method of Particle Swarm Optimization (PSO). The developed IT tool was used to determine the parameters of heat treatment, which will ensure obtaining the expected value for hardness. In the first stage, the ADI cast iron heat treatment parameters proposed by the expert were used, in the next part of the experiment, the settings proposed by the system were used. Used of the proposed IT tool, it was possible to reduce the number of deficiencies by 3%. The use of the solver in the case of castings with a wall thickness of 25 mm and 41 mm allowed to indication of process parameters allowing to obtain minimum mechanical properties in accordance with the PN-EN 1564:2012 standard. The results obtained by the solver for the selected parameters were verified. The indicated parameters were used to conduct experimental research. The tests obtained as a result of the physical experiment are convergent with the data from the solver.

Keywords: Solver, ADI, Prediction, Decision tree

1. Introduction

IT solutions firmly rooted in foundries, positively affecting the efficiency of new product implementation and process flexibility. Included among others, CAM, CAD, CAE programs, programs simulating the pouring process, liquid metal control systems, metal coagulation curve analysis systems [1]. The solutions developed with the use of artificial intelligence are characterized by an increasingly better accuracy of predicting the analyzed features or properties [2]. Work is also underway on tools supporting foundries based on machine learning. These solutions differ from the

previously mentioned IT tools, having in common the participation of an expert or properly prepared data in the learning process. It should be noted, however, that there are many methods developing simultaneously and well-known methods such as the finite element method are used [3]. Their application may concern various areas of the foundry's activity, both technological issues, e.g. heat treatment, optimization of the solidification process, as well as production management. These solutions are part of the industrial revolution, which is also changing the operation of foundries [4-5]. The Industry 4.0 concept places great emphasis on flexibility in the production process, which results in new challenges for especially small and medium-sized foundries [6]. Obtaining high flexibility while maintaining high production efficiency is associated with the need to introduce IT systems at various levels of the organization. Production flexibility can also affect the production process, making it even more complex [7-8]. For many manufacturing methods, it is possible to accurately track each of the stages of production. This allows you to create a system supporting the production process not only integrated with each of the machines involved in the process, but with unambiguous identification of the detail at each of the stages of production. Such systems can be fed with highly reliable data [9]. When tracking and collecting data in foundries, the situation can be much more difficult. This applies in particular to the traceability of individual castings, the metal from which they were cast, and processes related to the processing of this metal. In many cases, it is necessary to introduce a separate IT tool enabling identification of the cast and related processes [10-11]. The recorded data from the casting production process may show large spreads and come from various sources. However, there are mathematical and numerical methods that can work in these conditions. This can be confirmed by expert systems supporting identification of defective castings that are already available for foundries. The need for such solutions is particularly important at the initial design stage of the casting process. IT systems can reduce the costs and time needed to introduce new products [12]. Work on decision support systems concerns many areas, such as welding, laser cutting, mental health. These systems prove useful in many cases [13-14]. The use of decision support systems is part of the assumption of industry 4.0, where the role of a human being is limited to the initial commissioning, supervision and technical maintenance [15]. Decision-making systems enable predictions and thus prevent shortages or failures [16].

Austempered ductile iron (ADI) belongs to the ductile cast iron (DI) family, which is subjected to heat treatment; i.e., austenitization followed by austempering (isothermal quenching). The structure of ADI cast iron consists of spheroidal graphite nodules embedded in a metallic matrix called ausferrite, which consists of ferrite plates surrounded by high-carbon austenite. However all the factors above play important role in shaping of the ADI's microstructure, the temperature of the isothermal quenching is the one of the most significant. The austempering step of the heat treatment is usually conducted in a molten salt bath in the temperature range of 250 – 400 °C. With the increase of the temperature the morphology and volume fraction of the matrix constituents change. While choosing the temperature of the process from lower range, i.e. 250 – 330 °C, very fine needle or plate-like ferrite precipitations are obtained and the high-carbon austenite fraction is very low. In addition to heat treatment parameters, the chemical composition and wall thickness of the casting are also important. Despite many studies, not all relationships between process parameters and ausferrite morphology or microstructure, and thus mechanical and functional properties, are explained [17-18]. A separate group are thin-walled castings, which are increasingly used in industrial solutions. Therefore, the study of the influence of wall thickness and the possibility of prediction in this area is an important research issue [19]. Numerous studies are carried out related to the optimization of the parameters of the manufacturing process for thin-walled castings with an ausferritic matrix [20]. This is a complex issue, because the impact of defects in the form of porosity and inclusions, which may be formed in thin-walled castings during mold pouring, is also important for the final mechanical properties [21]. The microstructure of ADI cast iron is sensitive to the parameters of the manufacturing process, which results in different mechanical properties [22]. For nodular cast iron, the number and size of graphite precipitates slightly affect the measurement of strength, while the effect of graphite morphology on elongation is significant [23]. The form of graphite may be significantly affected by parameters such as wall thickness and mold parameters, which affects the rate of solidification and cooling of the metal. The final mechanical parameters of ADI cast iron may also be affected by the type of matrix obtained [24-28]. Therefore, the influence of many factors at individual stages of casting production on the structure of ADI cast iron is important. There is a rich literature on the relationship between heat treatment and the resulting structure. Numerous works are also carried out on the optimization of mechanical properties. A significant amount of research is conducted towards the use of IT tools for thin-walled castings, allowing for the selection of selected process parameters in order to obtain the expected properties. At the same time, the selection of these parameters should make it possible to obtain as few defects as possible. On the basis of the authors' opinion and the lack of available solutions, it was decided to undertake work in order to create a tool supporting greater repeatability of the final parameters of castings (in our case hardness) and to reduce the number of experimental tests and the number of defects.

2. Materials and Methods

2.1 Experimental Methodology

The experimental melt was prepared in a 50-kg-capacity crucible with neutral lining using an electrical induction furnace of an intermediate frequency Radyne AMF 45/100. The furnace charge consisted of pig iron: 4.04% C, 0.77% Si, 0.03% Mn, 0.005% S, 0.043%P), Fe-Si75, Fe-Mn80, carburizer, technically pure Cu and Ni, home ductile iron scrap. After being melted at 1500 °C, the liquid metal was held for 2 minutes, than tapped at 1490 °C into the reaction chamber (FLOTRET process). In the FLOTRET process (Fig. 1) liquid metal flows through the reactor – first through the reaction chamber, where the speroidizing and inoculation agents are placed, than through mixing chamber into the ladle (fig. 2). An Fe-Si-Mg Elmag 5800 foundry alloy (44 to 48 % Si, 5.5 to 6.2 % Mg, 0.8 to 1.2 % Ca, 0.8 to 1.2 % RE, 0.4 to 1.0 % Al, bal Fe) was used for spheroidization, while Foundrysil (73 to 78 % Si, 0.75 to 1.25 % Ca, 0.75 to 1.25 % Ba, 0.75 to 1.25 % Al, bal Fe) was used for inoculation purposes. The cast iron was

poured at about 1420 °C into Y-block ingots (2, 3, 5 and 13 mm) in a green sand dried mould (Fig.3). The chemical composition of the research material obtained in this way is marked with No. 1 in Table 1. The pouring temperature of the melt was 1420 °C, melting was also carried out in a Radyne AMF 45/100 furnace. The risers of the wedges were cut off before heat treatment. The chemical composition of the obtained castings is presented in the table 1 (no. 2 and 3).

Fig. 1. Lquid cast iron drain

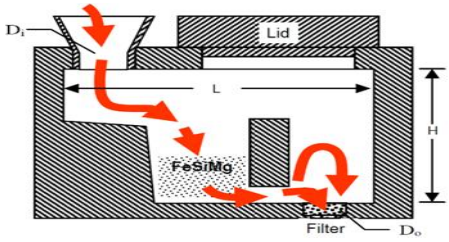

Fig. 2. Schematic drawing of reaction chamber

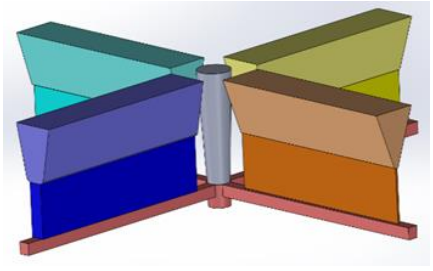

Fig. 3. Concept of model placement in a casting mold

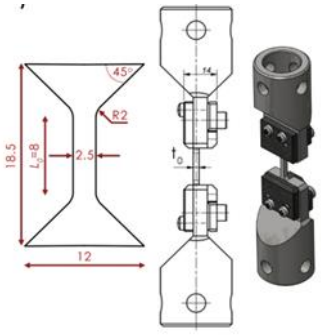

Fig. 4. Tensile testing sample dimensions

Even if the ADI cast iron production process is stable, there may be castings with significant fluctuation of properties resulting, among others, from variable wall thickness. The next stage of the research was the analysis of hardness distribution for castings with different walls subjected to heat treatment. The Łukasiewicz Research Network – Krakow Institute of Technology has a line for heat treatment required during the production of ADI cast iron. The line includes an austenitizing furnace, a hardening bath and a washer with a washer. The line enables processing of workpieces with a total weight of 250 kg at one time. Receiving in one time interval one range of castings, a hardness test was carried out on selected pieces from each of the lots. Obtaining hardness in the assumed range allowed for sending a given batch to the recipient. Hardness measurements were made on 57 castings. An example of the chemical composition of such an element is shown in Table 1 under number 3.

2.2. Materials

The obtained chemical composition of the ductile iron is presented in table 1.

Table 1
The chemical composition of ductile iron

	Chemical composition, wt. %									
No.	**C**	**Si**	**Mn**	**P**	**S**	**Mg**	**Cu**	**Ni**	**Mo**	**Cr**
1	3.3	2.6	0.2	0.055	0.006	0.04	0.8	1.5	no	0.05
2	3.6	2.45	0.32	0.04	0.015	0.065	0.93	1.9	no	0.03
3	3.57	2.13	0.74	0.06	0.015	0.038	0.7	1.2	0.2	0.02

The chemical composition tests of the experimental ductile iron were carried out using a GNR S3 MiniLab 300 emission spectrometer with spark excitation. The heat treatment for the ADI production consisted of austenitizing in a muffle furnace followed by austempering in a salt bath of NaNO2-KNO3 and finally air cooling to room temperature. Heat treatment parameters are presented in table 2.

Table 2.
Heat treatment parameters

	casting thickness mm	austenitization		austempering	
		tem. °C	time. h	tem. °C	time. h
0A	2-5	870	1	270	3
0B				390	1.5
1A	13		1.5	270	4
1B				390	2
2A	25	900	2	270	3
2B	25	900	2	375	2.5
3A	41	850	2	300	3
3B	30	860	2	390	2

Samples for mechanical testing and metallography were taken from castings. Due to the thickness of some castings equal or less than 5 mm, castings were ground to c.a. 2.5 mm thickness, than samples were cut out with the use of electro-spark wire cutting machine. Tensile testing was performed using Zwick Roell AllroundLine Z10 on flat samples with dimensions shown on figure 4. Hardness measurements were done using Zwick/Roell ZHU 250 hardness testing machine. Tests were carried out with accordance to appropriate standards: ISO 6892-1 / ISO 10113 / ISO 10275 for tensile testing and EN ISO 6506-1 for hardness measurements. All the mechanical properties of each thickness/heat treatment variant were determined on at least 3 samples. The metallographic examination was performed by optical microscope (Axio (New York, NY, USA) Observer. Z1m).

3. Solver details

3.1. Input data

The main component of the module for determining the parameters of the ADI manufacturing process for the production of products with specific properties is a solver based on the PSO method. It takes as input parameters:

- the wall thickness of the final product,
- ranges of the values of the elements characterizing the chemical composition of cast iron subjected to heat treatment in the ADI production process,
- value of hardness in Brinell scale (HB) for final product.

The wall thickness is selected by the user based on the GUI of the system. The ranges of the values of the elements correspond to the specific grade of ADI. The ADI grade is selected at an earlier stage of the decision system (without the use of a solver), which is influenced by the mechanical and performance properties of product selected by the user.

3.2. Material basics

The solver developed as part of this component is an algorithm that allows the calculation of the chemical composition parameters (C, Si, Mn, Ni, Mo, Cu, Mg) of cast iron subjected to heat treatment, the parameters of thermal treatment (austenitization and hardening temperatures) and value of HB. An important element of the solver is the equation developed by Voight and Loper [26] defining the critical diameter (G_{ws}) of the shaft, which ensures that such an element is hardened without the appearance of a pearlitic structure in its axial section. During the research leading to the development of this equation, isothermal hardening in a salt bath was used, similarly to that carried out in the Lukasiewicz Research Network - Krakow Institute of Technology. Thus, it was possible to verify the correctness of the results obtained when applying this equation.

As the result it was decided to implement the parameter modification C_x, which is the factor determining the content of carbon in austenite. There are equations linking C_x with the lattice parameters [27] as well as with specific process parameters [28], this is a difficult issue to quantify under production conditions. In the proposed model, two equations were used to calculate C_{x1} and C_{x2}. This modification allows for better predictions as compared to the results obtained by using only the C_{x1} parameter. This may be due to the fact that the equation describing C_{x1} is defined for Fe-C-Si alloys. The final formula for defining the formula for the wall thickness along with the modifications made is presented in equation.

$$G_{ws}=(124*C_x)+(27*Si)+(22*Mn)+(16*Ni)-(25*Mo)-(1{,}68*10^{-4}*T_{h2})+(12*Cu*Ni)+(62*Cu*Mo)+(88*Ni*Mo)+(11*Mn*Cu)+(127*Mn*Mo)-(20*Mn*Ni)-137$$

where:
$C_x = (C_{x1}+C_{x2})/2$ - estimated content of carbon in austenite,
C_{x1}= Ta/420-(0,17*Si)-0,95)
$C_{x2}=(-0.435+((0.335*10^{-3})*T_a)+((1{,}61*10^{-6})*T_{a2})+(0.006*Mn)$ - - (0.11*Si)-(0.07*Ni)+ +(0.014*Cu)-(0.3*Mo)
T_h - hardening temperature,
T_a - austenitizing temperature.

The equation is a crucial component of the solver, which, together with the rules defining the range of heat treatment parameters used, and the product wall thickness enables the manufacturing products with appropriate mechanical and performance properties. Equation works well in certain ranges of variable values, depending on e.g. on ADI grade and empirical experiences. It is therefore all the more necessary to use the maximum and minimum values for the chemical elements and the parameters of the heat treatment process, resulting from the literature review and from the experience gained during the production of ADI. In the case of determining the carbon content, the calculations were based on the wall thickness of the casting and the formula for the carbon equivalent based on the Si content previously calculated by the solver, as shown in table 3.

Table 3.
The content of carbon in the alloy depending on the wall thickness and silicon content [29].

Gws [mm]	x ≤ 13	13 < x < 51	51 ≤ x
C	4,4 – (⅓*Si)	(4,6-⅓*Si)	4,5-⅓*Si

In practical applications, there may be a situation where it is not possible to change the chemical composition of the ductile cast iron

(subjected to heat treatment process), so it is only possible to modify the heat treatment parameters. In this case, both the content of carbon and other elements must remain constant and comply with the provided certificate of chemical composition. Such functionality has been provided and based on the equation 1, taking into account the Max and Min ranges for the elements Si, Mn, Ni, Mo, Cu, temperatures hardening temperature (T_h) and temperature austenitization (T_a) (presented in table 4), the wall thickness of the casting and the adopted carbon equivalent for the given thicknesses walls, appropriate parameters are calculated using the particle swarm method. Depending on the needs, these parameters may include: percentage composition of elements, austenitization and austempering. It should be noted that the given formula is not a unimodal function, i.e. the desired wall thickness can be obtained for various sets of parameters for strictly defined ranges of elements and temperatures

Table 4.
Ranges of values chemical composition

	Chemical composition % by weight						Process Temperature °C	
	C	Si	Mn	Ni	Mo	Cu	T_h	T_a
Min	3.4	2.1	0.2	0	0	0	270	830
Max	3.8	2.7	0.35	2.0	0.2	0.8	390	950

Value of HB was define based on three presented in figure 4.

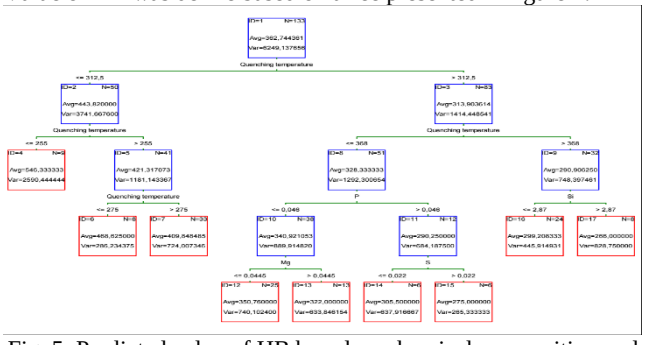

Fig. 5. Predicted value of HB based on chemical composition and hardening temperature

Based on this tree it is possible to set range of Mg, S, P, Si and the hardening temperature for define HB value. Mg and P content are not used to calculate G_{ws}. In this solution content of phosphorus was set as 0.043, while magnesium content is calculated based on an empirical formula, shown under:

Mg=(((DefHB-1615.16-(-6.10*T_h(i))- (0.0069* T_h(i)* T_h(i)) –(-872.90*P(i){0.043}*Ni(i))))/((1032.1532*Cu(i)))
based where:
DefHB – define value of HB for final product.

3.3. Implementation details

The input parameters of the solver are the limit ranges (chemical composition) determined at the previous stage of the system operation and the target wall thickness and HB of the product determined by the user. The method used to implement the solver is the method of Particle Swarm Optimization (PSO) based on the observation of nature, described in detail by Sztangret et at. [29]. The particles (identifying the solution to the problem under study) move the decision space (the area inhabited by the population) tracking the particle representing the best solution so far. Each particle is represented by two vectors - the position vector of the particle and the velocity vector of the particle. Particle swarm initialization is based on generating a random particle position (maximum and minimum content of alloying elements { Si, Mn, Ni, Mo, Cu, Th, and Ta) and particle velocity as 5% of the difference between the maximum and minimum value of the alloying elements. The new value of velocity vector is calculated based on the following relation**:**

$$v_{k+i}^{i} = wv_k^i + r_1\left(p^q - x_k^i\right) + r_2\left(p^i - x_k^i\right)$$

where:
v_{k+i}^{i} - velocity in k+1 iteration,
$v_k{}^i$- velocity in k iteration,
$x_k{}^i$- position vector,
p^g- the best position of all swarm particles,
p^i- the best solution found from the whole swarm by particle i,
r_1, r_2 - coefficients generated randomly from the range [0,1],
w - inertia coefficient chosen from the range [0,1] (for this solution w=0.8)

The new position of the particle is determined from the Eq.4:

$$x_{k+1}^{i} = k_{k+1}^{i} + v_{k+1}^{i}$$

The objective function is calculated for all particles i from the:

$$f(i) = abs(C_{ws}(i) - G_{ws}) + abs(HB(i) - DefBH)$$

where:
C_{ws}(i)- calculated wall size for i-th particle, G_{ws}- expected wall size, HB(i) – calculated value of HB for i-th particle.

The flowchart of PSO algorithm was in Figure 6. W When the calculated wall thickness for particle i is less than the assumed one, a penalty function is introduced into the objective function (adding a value of 10 to the objective function). Such a procedure means that even though the particle may have a low value of the objective function this solution will not be taken as correct by the solver. The value of the objective function less than 0.01 was defined as a stopping criterion of optimization algorithm. This value corresponds to the difference of the wall thickness assumed in the algorithm to the wall thickness determined by the algorithm.

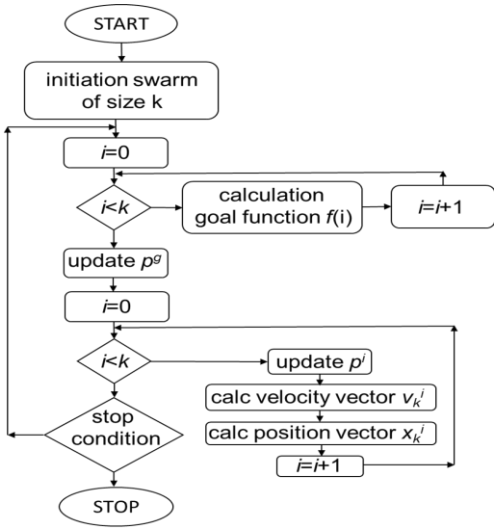

Fig. 6. The flowchart of PSO algorithm

Figure 7 shows the value of the objective function, Ni content, hardening and austenitizing temperature during the three runs of the optimization algorithm. As can be seen from the analysis, the algorithm converges quickly (less than 20 runs) and finds the assumed goal function.

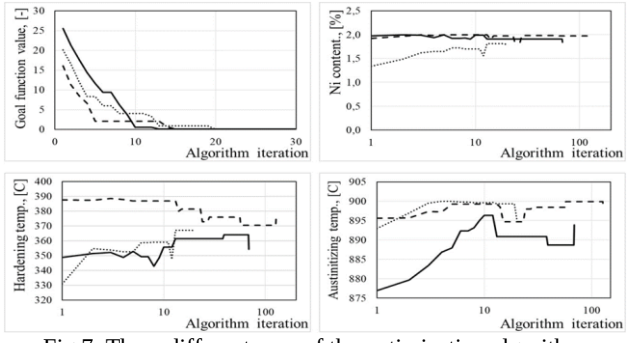

Fig 7. Three different runs of the optimization algorithm

4. Results and Discussion

The developed IT tool was used to determine the parameters of heat treatment, which will ensure obtaining the expected value for hardness. In the first stage, the ADI cast iron heat treatment parameters proposed by the expert were used, in the next part of the experiment, the heat treatment parameters proposed by the system were used. The results obtained are shown in Figure 8. Expert proposition was mark as "a" on hardness distribution histogram. From the presented distribution it can be see that about 13% of measurements exceed the permissible hardness range for those elements. The distribution marked with the symbol "b" shows the hardness distribution after entering the heat treatment proposed by the IT tool. The number of elements exceeding the designated hardness limits (250 HB - 280 HB) was limited to 10%. It should be noted that a greater concentration of particularly expected hardness's in the range of 260 HB to 270 HB was obtained than was the case with the heat treatment parameters proposed in the first part of the experiment.

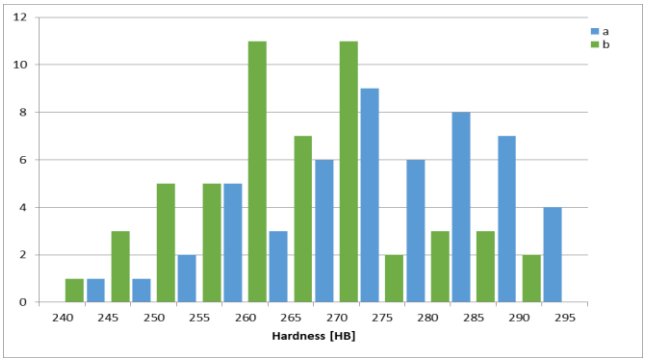

Fig. 8. Histogram of ADI cast iron hardness distribution a) expert proposition; b) Decision support system proposition

The wall thickness of the elements (3B), whose hardness distribution is shown in figure 8 is 30 mm, in the case of samples 0 and 1, the thickness of the wall hardness is 5 mm and 13 mm, respectively. For these samples, the discussed IT tools were not used to determine the heat treatment parameters. In the case of samples 2 and 3, the applied heat treatment was carried out in accordance with the results obtained from the developed IT tool. The results of the mechanical properties obtained are presented in the table 5.

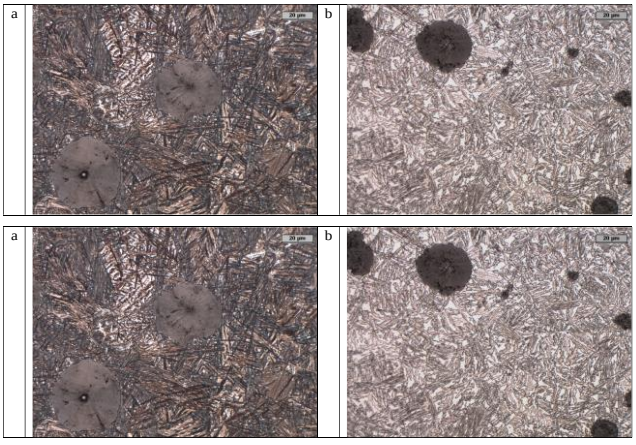

Fig. 9. Depicts the microstructure of ADI cast iron austempered at a) 270 °C (lower ausferrite) and b) 390 °C (upper ausferrite).

Figure 9 show microstructure sample 0 after heat treatment according table 2. In the case of lower ausferrite, large number of needle-like ferrite precipitations (dark phase) are observed and the high-carbon austenite (white phase) fraction is very low. On the other hand, upper ausferrite is characterized by much lower number of ferrite feathery-like precipitations with higher thickness and the fraction of high-carbon austenite is significantly higher. Figure 10 shows the microstructure of samples 2 and 3. Sample 2A contains a small amount of high-carbon austenite compared to sample 2B. A significant amount of austenite is incorporated in sample 3A.

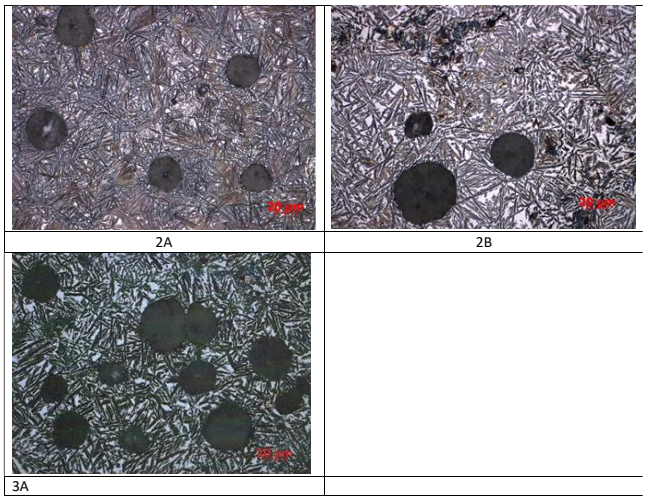

Fig. 10. The microstructure of the samples 2 and 3 after heat treatment according table 2.

Table 5 presents the results of selected mechanical properties of some of the tested alloys. In the case of sample 0 A and 2 A alloys, isothermal quenching was carried out at 270°C. For hardness, the difference between sample 0A and 2A is 101 HB, which is a real difference. In the case of such a low hardness, it is also difficult to explain the obtained elongation and tensile strength. The sample marked with the symbol 0B reached an elongation of 6.4%, which is a significantly lower value compared to sample 2B. Based on the PN-EN 1564:2012 standard, it can be stated that in the case of samples 2 and 3, the expected properties were obtained.

Table 5
Mechanical properties of selected alloys

	Thickness of the wall [mm]	UTS, MPa	YS, MPa	A, %	HB [-]	KC [J]
0A	3-5	1396	1114	1.9	300	-
0B	3-5	895	684	6.4	-	-
2A	25	1480	1130	2.4	401	54.5
2B	25	950	580	8.2	264	80.6
3A	41	1430	1280	1.7	360	56.1

5. Conclusions

The use of modern IT tools is a common practice in foundries, and development of these solutions should also be expected. The development of the proposed tool may include thin-walled castings. Based on the obtained results, it can be concluded that:

1. Thanks to the use of the proposed IT tool, it was possible to reduce the number of deficiencies by 3%.
2. The use of the solver in the case of castings with a wall thickness of 25 mm and 41 mm allowed to obtain tensile strength and elongation accordance with the PN-EN 1564:2012 standard.

The properties of ADI cast iron are significantly affected by the microstructure of the initial cast iron described in the article and the time of isothermal cooling, the so-called "transformation time window. The authors intend to take this aspect into account when developing appropriate algorithms in further work.

Acknowledgements

The presented research was carried out as part of the research and development project entitled "The innovative process of cast iron castings production with the use of an intelligent informational managing system" (POIR.01.02.00-00-0248/16) co-financed by the National Center for Research and Development from the funds of the Operational Program Intelligent Development - Action Projects B+ R enterprises, Sub-measure Industrial research and development works carried out by enterprises.

References

[1] Šabík, V., Futáš, P. & Pribulová, A. (2022). Failure analysis of a clutch wheel for wind turbines with the use of casting process simulation. *Engineering Failure Analysis*. 135, 106159. DOI:10.1016/J.ENGFAILANAL.2022.106159.
[2] Shahane, S., Aluru, N., Ferreira, P., Kapoor, S.G. & Vanka, S.P. (2020). Optimization of solidification in die casting using numerical simulations and machine learning. *Journal of Manufacturing Process*. 51, 130-141, DOI:10.1016/J.JMAPRO.2020.01.016.
[3] Miller, S.W., Finke, D.A., Kupinski, M. & Ligetti, C.B. (2019). WeldANA: welding decision support tool for conceptual design. *Journal of Manufacturing Systems.* 51, 120-131. DOI:10.1016/J.JMSY.2019.04.007.
[4] Del Vecchio, C., Fenu, G., Pellegrino, F.A., Michele, D.F., Quatrale, M., Benincasa, L., Iannuzzi, S., Acernese, A., Correra, P. & Glielmo, L. (2019). Support vector representation machine for superalloy investment casting optimization. *Applied Mathematical Modeling*. 72, 324-336. DOI:10.1016/J.APM.2019.02.033.
[5] Sukhodolov, Y.A. The notion, essence, and peculiarities of industry 4.0 as a sphere of industry. undefined 2018, 169, 3-10. DOI:10.1007/978-3-319-94310-7_1.
[6] Kozłowski, J., Sika, R., Górski, F., Ciszak, O. (2019). Modeling of foundry processes in the era of industry 4.0. *Advances in lecture notes in mechanical engineering; Pleiades Publishing.* 62-71. DOI:10.1007/978-3-319-93587-4_7.
[7] Stawowy, A., Duda, J. & Wrona, R. (2016). Applicability of business rules to production management in foundries. *Archives of Foundry Engineering*. 16(1), 85-88. DOI:10.1515/afe-2016-0008.
[8] Mumali, F. (2022). Artificial neural network-based decision support systems in manufacturing processes: a systematic literature review. *Computers & Industrial Engineering.* 165, 107964. DOI:10.1016/J.CIE.2022.107964.
[9] Yang, D.Y., Bambach, M., Cao, J., Duflou, J.R., Groche, P., Kuboki, T., Sterzing, A., Tekkaya, A.E. & Lee, C.W. (2018). Flexibility in metal forming. *CIRP Annals*. 67(2), 743-765, DOI:10.1016/j.cirp.2018.05.004.

[10] Uyan, T., Otto, K., Silva, M.S., Vilaça, P. & Armakan, E. (2023). Industry 4.0 foundry data management and supervised machine learning in low-pressure die casting quality improvement. *International Journal of Metalcasting*. 17(1), 414-429. DOI:10.1007/S40962-022-00783-Z/TABLES/3.
[11] Wadhwa, R.S. (2013). Methodology for internal traceability support in foundry manufacturing. In IFIP Advances in Information and Communication Technology, 9-12 September 2013 (pp. 183-190). Berlin, Heidelberg: Springer.
[12] Iqbal, M.F., Javed, M.F., Rauf, M., Azim, I., Ashraf, M., Yang, J., & Liu, Q.-feng (2021). Sustainable utilization of foundry waste: forecasting mechanical properties of foundry sand based concrete using multi-expression programming. *Science of the Total Environment*. 780(1), 146524. DOI:10.1016/J.SCITOTENV.2021.146524.
[13] Lutz, W., Deisenhofer, A.K., Rubel, J., Bennemann, B., Giesemann, J., Poster, K. & Schwartz, B. (2021). Prospective evaluation of a clinical decision support system in psychological therapy. *Journal of Consulting and. Clinical Psychology*. 90(1), 90-106. DOI:10.1037/CCP0000642.
[14] Abdelsadek, Y. & Kacem, I. (2022). Productivity improvement based on a decision support tool for optimization of constrained delivery problem with time windows. *Computers & Industrial Engineering*. 165, 107876. DOI:10.1016/J.CIE.2021.107876.
[15] Stanek K. (2020). Case studies in foundry 4.0. Modern Casting, April. 32-36.
[16] Kopper, A.E. & Apelian, D. (2022). Predicting quality of castings via supervised learning method. *International Journal of Metalcasting*. 16(1), 93-105. https://doi.org/10.1007/s40962-021-00606-7.
[17] Gazda, A., Warmuzek, M. & Bitka, A. (2018). Optimization of mechanical properties of complex, two-stage heat treatment of Cu–Ni (Mn, Mo) austempered ductile iron. *Journal of Thermal Analysis and Calorimetry*. 132, 813-822. https://doi.org/10.1007/s10973-018-7004-6.
[18] Jhaveri, K., Lewis, G.M., Sullivan, J.L. & Keoleian, G.A. (2018). Life cycle assessment of thin-wall ductile cast iron for automotive lightweighting applications. *Sustainable Materials and Technologies.* 15, 1-8, DOI:10.1016/J.SUSMAT.2018.01.002.
[19] Almanza, A., Dewald, D., Licavoli, J. & Sanders, P.G. (2021). Effect of cobalt additions on the microstructure and mechanical properties of as-cast thin-wall ductile iron. *International Journal of Metalcasting*. 15(2), 417-432. https://doi.org/10.1007/s40962-020-00513-3.
[20] Sarkar, T. & Sutradhar, G. (2018). Investigation into the microstructure and mechanical properties of thin wall austempered gray cast iron (TWAGI). *Transactions of the Indian Institute of Metals*. 71, 2133-2143. https://doi.org/10.1007/s12666-018-1345-5.
[21] van gen Hassend, F., Ninnemann, L., Töberich, F., Breuckmann, M., Röttger, A., Weber, S. (2022). Study on the austemperability of thin-wall ductile cast iron produced by high-pressure die-casting. *Journal of Materials Engineering and Performance*. 31, 1405-1418. https://doi.org/10.1007/s11665-021-06252-8.
[22] Wang, X., Du, Y., Liu, C., Hu, Z., Li, P., Gao, Z., Guo, H. & Jiang, B. (2022). Relationship among process parameters, microstructure, and mechanical properties of austempered ductile iron (ADI). *Materials Science and Engineering: A.* 857, 144063. https://doi.org/10.1016/j.msea.2022.144063.
[23] Liu, C., Du, Y., Ying, T., Zhang, L., Zhang, X., Wang, X., Yan, G. & Jiang, B. (2022). Effects of graphite nodule count on mechanical properties and thermal conductivity of ductile iron. *Materials Today Communications.* 31, 103522. https://doi.org/10.3390/lubricants10120326.
[24] Sellamuthu, P., Samuel, D.G.H., Dinakaran, D., Premkumar, V.P., Li, Z. & Seetharaman, S. (2018). Austempered ductile iron (ADI): influence of austempering temperature on microstructure. *Mechanical and Wear Properties and Energy Consumption. Metals.* 8(1), 53, 1-12. DOI:10.3390/MET8010053.
[25] Voigt, R.C. & Loper, C.R. (1984). Austempered ductile iron—process control and quality assurance. *Journal of Heat Treating*. 3, 291-309. DOI:10.1007/BF02833124.
[26] Sun, X., Wang, Y., Li, D.Y. & Wang, G. (2013). Modification of carbidic austempered ductile iron with nano ceria for improved mechanical properties and abrasive wear resistance. *Wear*. 301(1-2), 116-121. DOI:10.1016/J.WEAR.2012.12.018.
[27] Zahiri, S.H., Pereloma, E.V., Davies, C.H.J. (2013). Application of bainite transformation model to estimation of processing window boundaries for Mn-Mo-Cu austempered ductile iron. *Materials Science and Technology.* 17(12), 1563-1568. http://dx.doi.org/10.1179/026708301101509610.
[28] David, P., Massone, J., Boeri, R. & Sikora, J. (2004). Mechanical properties of thin wall ductile iron-influence of carbon equivalent and graphite distribution. *ISIJ Int*ernational. 44(7), 1180-1187, DOI: 10.2355/ISIJINTERNATIONAL.44.1180.
[29] Sztangret, Ł., Stanisławczyk, A. & Kusiak, J. (2009). Bio-inspired optimization strategies in control of copper flash smelting process. *Computer Methods in Materials Science.* 9(3), 400-408.